Microscopic structure of low-lying positive parity states in nuclei near shell closure

N. Lo Iudice
Dipartimento di Scienze Fisiche, Universitá di Napoli Federico II and Istituto Nazionale di Fisica Nucleare, Sezione di Napoli Complesso Monte S. Angelo, via Cintia I-80126, Napoli, Italy

Ch. Stoyanov
Institute for Nuclear Research and Nuclear Energy, 1784 Sofia, Bulgaria
(Received 4 July 2001; published 23 May 2002)

We adopt the quasiparticle-phonon model to investigate the microscopic structure of some low-lying states recently discovered in nuclei around shell closure. The study determines quantitatively the phonon content of these states and shows that their main properties are determined by a subtle competition between particle-particle and particle-hole quadrupole interactions and by the interplay between orbital and spin-flip motion. The results are in overall agreement with experiments and consistent with the interacting boson model and shell model calculations.

DOI: 10.1103/PhysRevC.65.064304 PACS number(s): 21.60.Ev, 23.20.−g, 27.60.+j

I. INTRODUCTION

Considerable effort has been devoted to the search and study of low-lying states in heavy nuclei after the discovery of the magnetic dipole ($M1$) excitation in the deformed ^{156}Gd through inelastic electron scattering experiments [1]. Such a mode, known as scissors mode, was predicted for deformed nuclei in a semiclassical two-rotor model [2], in schematic microscopic approaches [3,4], and in the proton-neutron version of the interacting boson model (IBM-2) [5,6]. As discussed in several reviews [7–9], this $M1$ mode is now well established in the different deformed regions of the periodic table and is also fairly well understood on experimental as well as theoretical grounds. A remarkable property that links its occurrence to deformation is the strict correlation between the total $M1$ strength and the $E2$ strength collected by the first 2^+ rotational state [10–15].

Another important feature of the scissors mode is its isovector character. States of isovector nature were first considered in a geometrical model [16] as proton-neutron surface vibrational high-energy modes. These states were predicted to exist also at low energy in a revised version of the model [17,18]. Low-lying isovector excitations are naturally predicted in the algebraic IBM-2 as mixed symmetry states with respect to the exchange between proton and neutron bosons. They are distinguished from the symmetric ones by the F-spin quantum number [19], which is the boson analog of isospin for nucleons. The symmetric states have maximum F spin, $F=F_{max}=(N_\pi+N_\nu)/2$, where N_π and N_ν are, respectively, the number of proton and neutron bosons. The lowest mixed-symmetry states have $F=F_{max}-1$. Their main signatures are relatively weak $E2$ and strong $M1$ transitions to symmetric states. Indeed, the scissors mode was identified in deformed nuclei through its $M1$ excitation from the ground state.

In spherical nuclei, the $M1$ excitation mechanism cannot be claimed to generate the scissors mode and, more generally, mixed symmetry states from the $J^\pi=0^+$ ground state, because of the conservation of the angular momenta of proton and neutron fluids. In these nuclei, the lowest mixed-symmetry state is predicted to have $J^\pi=2^+$ and can be excited from the ground state via weak $E2$ transitions. Its signature, however, is its strong $M1$ decay to the lowest isoscalar $J^\pi=2^+$ state.

Due to the difficulty of a direct excitation from the ground state, the mixed-symmetry states in spherical or nearly spherical nuclei eluded the experimental observation for several years. The evidence for their existence was deduced from the small measured $E2/M1$ mixing ratio [20,21], from inelastic hadron scattering cross sections [22], and from the measurements of the electron conversion coefficients in β decay [23]. The mixed symmetry character of these states was confirmed in lifetime measurements, which allowed to determine the strength of the $M1$ transition to the lowest 2^+ state [24–28].

Recently, however, unambiguous evidence in favor of mixed-symmetry states was provided by an experiment that combined photon scattering with a $\gamma\gamma$-coincidence analysis of the transitions following β decay of ^{94}Tc to ^{94}Mo [29]. Such a decay has populated several excited states among which it was possible to identify a two-phonon $J^\pi=1^+$ and a one-phonon $J^\pi=2^+$ mixed-symmetry states. The picture was enriched with the subsequent identification of two additional mixed symmetry states, a $J^\pi=3^+$ [30] and a $J^\pi=2^+$ [31] two-phonon states. These experiments have also produced an almost exhaustive mass of information on low-lying levels and absolute transition strengths, which made possible a rather accurate characterization of these low-lying states. This analysis was carried out in IBM-2 and could test not only the F spin character of the states, but also the multiphonon content of them. It was found that, while the lowest mixed-symmetry $J^\pi=2^+$ state is composed of a single phonon, the other states lying at higher energy have a two phonon structure.

The collectivity and the energy of the low-lying excitations in nuclei near shell closure change considerably with A. This reflects the high sensitivity of the simple (collective and non collective) modes to the detailed shell structure of the system. The phenomenological algebraic model is not suitable for clarifying this structure. Such a task is demanded to

microscopic approaches. Two microscopic calculations have been carried out so far. One was framed within the nuclear shell model [32], the other within the quasiparticle-phonon model (QPM) [33]. The two approaches are complementary under many respects. The shell model provides naturally information on the single-particle content of the wave function. Moreover it is exact within the chosen model space. On the other hand, the space truncation induces uncertainties and, in this specific case, can account only effectively for the coupling between the low-lying, mainly orbital, states under study and the spin-flip configurations that are partly excluded from the model space.

The spherical QPM [34] is based on the quasiboson approximation typical of the random-phase approximation (RPA) and, therefore, is reliable only in spherical nuclei with few valence nucleons. On the other hand, it allows to choose the configurations that are more relevant to the problem, including the high-energy spin-flip configurations, and has a clear phonon content, which allows to state a bridge with the IBM-2 analysis. Microscopic states incorporating proton neutron out of phase quadrupole correlations, which may be viewed as microscopic counterparts of the IBM mixed-symmetry states, were envisaged long ago in an anharmonic extension of RPA [35].

In Ref. [33], the QPM calculation confirmed the picture provided by IBM-2 for the low-energy spectrum of ^{94}Mo. It was necessary, however, to use a quite small spin gyromagnetic factor to suppress the spin contribution. In this paper we reexamine the adopted scheme in order to try to get a more consistent description of the spectrum. We also make a systematic study of the low-lying spectra in nuclei near different shell closures and compare the results to the available experimental data. Such a study should put on display the features common to the spectra in different nuclei but should also explain their differences in terms of the peculiar shell structure of each nucleus.

II. BRIEF OUTLINE OF THE QPM

We considered an intrinsic Hamiltonian having the following structure:

$$H = H_{sp} + V_{pair} + V_M^{ph} + V_{SM}^{ph} + V_M^{pp}. \tag{2.1}$$

H_{sp} is a one-body Hamiltonian, V_{pair} the monopole pairing, V_M^{ph} and V_{SM}^{ph} are, respectively, sums of particle-hole separable multipole and spin-multipole interactions, and V_M^{pp} is the sum of particle-particle multipole pairing potentials.

Following the QPM procedure, we transformed the above Hamiltonian into a multiphonon one of the form

$$H_{QPM} = \sum_{i\mu} \omega_{i\lambda} Q^\dagger_{i\lambda\mu} Q_{i\lambda\mu} + H_{vq}, \tag{2.2}$$

where the first term is the unperturbed phonon Hamiltonian and H_{vq} is a phonon-coupling piece whose exact expression can be found in Ref. [34]. Both terms are expressed in terms of the RPA phonon operators

$$Q^\dagger_{i\lambda\mu} = \frac{1}{2} \sum_{jj'} \{\psi^{i\lambda}_{jj'} [\alpha^\dagger_j \alpha^\dagger_{j'}]_{\lambda\mu} - (-1)^{\lambda-\mu} \varphi^{i\lambda}_{jj'} [\alpha_{j'} \alpha_j]_{\lambda-\mu}\}_\tau \tag{2.3}$$

of multipolarity $\lambda\mu$ and energy $\omega_{i\lambda}$, where $\alpha^\dagger_{jm}(\alpha_{jm})$ are quasiparticle operators obtained from the corresponding particle operators through a Bogoliubov transformation. The phonon operators fulfill the normalization conditions

$$\frac{1}{2} \sum_{jj'} [\psi^{i\lambda}_{jj'} \psi^{i'\lambda'}_{jj'} - \varphi^{i\lambda}_{jj'} \varphi^{i'\lambda'}_{jj'}] = \delta_{ii'} \delta_{\lambda\lambda'}. \tag{2.4}$$

It is worth pointing out that the RPA phonon basis includes collective as well as noncollective phonons. The first ones are coherent linear combinations of many quasiparticle pair configurations. The lowest $[2^+_1]_{RPA}$ and $[3^-_1]_{RPA}$ phonon states are notable examples. Most of the states, however, are noncollective phonons, namely, pure two-quasiparticle configurations. It is also important to stress that the particle-particle interaction V_M^{pp} is included in generating the RPA solutions. Such a term enhances the particle-particle correlations in the phonons and will be shown to play a crucial role.

We finally put the quasiparticle-phonon Hamiltonian in diagonal form by using the variational principle with a trial wave function of total spin JM [36–38]

$$\Psi_\nu(JM) = \Bigg\{ \sum_i R_i(\nu J) Q^\dagger_{iJM} + \sum_{\substack{i_1\lambda_1 \\ i_2\lambda_2}} P^{i_1\lambda_1}_{i_2\lambda_2}(\nu J) \times [Q^\dagger_{i_1\lambda_1} \otimes Q^\dagger_{i_2\lambda_2}]_{JM} + \sum_{\substack{i_1\lambda_1 i_2\lambda_2 \\ i_3\lambda_3 I}} T^{i_1\lambda_1 i_2\lambda_2 I}_{i_3\lambda_3}(\nu J) \times [[Q^\dagger_{i_1\lambda_1} \otimes Q^\dagger_{i_2\lambda_2}]_I \otimes Q^\dagger_{i_3\lambda_3}]_{JM} \Bigg\} \Psi_0, \tag{2.5}$$

where R, P, and T are unknown amplitudes, and ν labels the specific excited state. The phonon operators (2.3) fulfill the exact commutation relations [34,36–38]

$$[Q_{i\lambda\mu}, Q^\dagger_{i'\lambda'\mu'}] = \frac{\delta_{i,i'}\delta_{\lambda,\lambda'}\delta_{\mu,\mu'}}{2} \sum_{jj'} [\psi^{i\lambda}_{jj'} \psi^{i'\lambda}_{jj'} - \varphi^{i\lambda}_{jj'} \varphi^{i'\lambda}_{jj'}] - \sum_{\substack{jj'j_2 \\ mm'm_2}} \alpha^+_{jm} \alpha_{j'm'} \{\psi^{i\lambda}_{j'j_2} \psi^{i'\lambda'}_{jj_2} C^{\lambda\mu}_{j'm'j_2m_2} \times C^{\lambda'\mu'}_{jmj_2m_2} - (-)^{\lambda+\lambda'+\mu+\mu'} \times \varphi^{i\lambda}_{jj_2} \varphi^{i'\lambda'}_{j'j_2} C^{\lambda-\mu}_{jmj_2m_2} C^{\lambda'-\mu'}_{j'm'j_2m_2}\}. \tag{2.6}$$

While the first term corresponds to the boson approximation, the second takes into account the internal fermion structure of phonons and ensures the antisymmetrization of the multiphonon wave function (2.5) and is of great importance for computing the electromagnetic transitions.

TABLE I. The parameters of the Woods-Saxon potential.

Nucleus		r_0 (fm)	V_0 (MeV)	κ (fm^2)	α (fm^{-1})
^{136}Ba	N	1.28	43.40	0.413	1.613
	Z	1.31	53.43	0.349	1.538
^{94}Mo	N	1.29	44.70	0.413	1.613
	Z	1.24	56.86	0.338	1.587

The response to electromagnetic external fields is computed by using a transition operator composed of two pieces [37],

$$M(X\lambda\mu)=M^{(ph)}(X\lambda\mu)+M^{(sc)}(X\lambda\mu). \tag{2.7}$$

The first term

$$M^{(ph)}(X\lambda\mu)=\frac{1}{2\sqrt{2\lambda+1}}\sum_{ijj'}\langle j||X\lambda||j'\rangle u^{(\pm)}_{jj'}(\psi^{i\lambda}_{jj'}+\varphi^{i\lambda}_{jj'}) \times[Q^{\dagger}_{i\lambda\mu}+(-)^{\lambda-\mu}Q_{i\lambda-\mu}] \tag{2.8}$$

promotes the exchange of one phonon between initial and final states. The second

$$M^{(sc)}(X\lambda\mu)=\frac{1}{\sqrt{2\lambda+1}}\sum_{jj'}\langle j||X\lambda||j'\rangle v^{(\mp)}_{jj'}[\alpha^{+}_{j}\otimes\alpha_{j'}]_{\lambda\mu} \tag{2.9}$$

was introduced in Ref. [37] and induces the so-called *boson forbidden* transitions between components with the same number of phonons or differing by an even number of them. The factors

$$u^{(\pm)}_{jj'}=u_j v_{j'}\pm v_j u_{j'},$$
$$v^{(\pm)}_{jj'}=u_j u_{j'}\pm v_j v_{j'} \tag{2.10}$$

appearing in the above equations are induced by the Bogoliubov transformation and renormalize the single-particle reduced transition matrix elements $\langle j||X\lambda||j'\rangle$.

III. NUMERICAL DETAILS

We fixed the parameters of the Hamiltonian according to a procedure well established in QPM, which yields a well defined set of parameters for all nuclei of a given nuclear mass region, valid for high- as well low-energy spectroscopic studies [34,36–39].

More specifically, we adopted a Woods-Saxon one-body potential U with parameters taken from [40,41] and shown in Table I. The corresponding single-particle spectra can be found in Ref. [39]. The single-particle space encompasses all shells below as well as all bound states above the Fermi energy. By virtue of such a large basis, which allows for excitations of valence and core nucleons, the quasiparticle space is much larger than the one covered by the valence nucleon states only.

We used a monopole pairing with a strength constant fixed so as to reproduce the experimental odd-even mass difference. For the other multipole fields entering into the particle-hole and particle-particle separable interactions we adopted the radial dependence $f(r)=dU(r)/dr$. We fixed the isoscalar strengths $\kappa_0^{(2)}$ and $\kappa_0^{(3)}$ of the quadrupole-quadrupole and octupole-octupole particle-hole interaction by a fit to the energies of the first collective 2^+ and 3^- states carried out in QPM (rather than RPA). We cannot apply the same prescription to the higher multipoles because of the absence of low-lying one-phonon collective states of the corresponding multipolarity. Rather than introducing new arbitrary parameters, we have adopted, as common practice in QPM, vanishingly small isoscalar strengths $\kappa_0^{(\lambda)}$ so as to leave unchanged the energy of the computed lowest two-quasiparticle states [39]. This prescription yields noncollective one-phonon states, which are practically pure two-quasiparticle states. The lack of experimental information does not allow one to fit the isovector constants to known levels. We have, therefore, taken all of them in the ratio $\kappa_1^{(\lambda)}/\kappa_0^{(\lambda)}=-1.5$ with the corresponding isoscalar constants, a value determined for the electric dipole modes in the QPM analyses. This ratio is smaller than the value deduced from the symmetry energy [42], but close to the one obtained in recent critical analyses about the choice of these isovector strengths [43,44]. The only spin-multipole relevant to our problem is the spin-spin interaction. The isovector constant of this interaction was deduced from the measured peaks of Gamow-Teller resonances observed in ^{90}Zr while the isoscalar one was taken very small, a choice widely adopted in QPM as well as in RPA and consistent with estimates based on sum-rule prescriptions [45]. The multipole pairing interaction, first analyzed by Belyaev [46], was shown to be necessary to the restoration of the Galilean invariance broken by the monopole pairing [46–48]. We used only a quadrupole pairing with strength parameters $G^{(2)}=G^{(2)}_{nn}=G^{(2)}_{pp}$ and $G^{(2)}_{np}=0$. This is enough for our purposes.

We studied first the properties of the first and second 2^+ RPA states, which are expected to represent the building blocks of the low-lying multiphonon states. To this purpose we have computed the ratio [49]

$$B(2^+)=\frac{\left|\langle 2^+\|\sum_k^p r_k^2\,Y_2(\Omega_k)-\sum_k^n r_k^2\,Y_2(\Omega_k)\|\text{g.s.}\rangle\right|^2}{\left|\langle 2^+\|\sum_k^p r_k^2\,Y_2(\Omega_k)+\sum_k^n r_k^2\,Y_2(\Omega_k)\|\text{g.s.}\rangle\right|^2} \tag{3.1}$$

to probe the isoscalar $[B(2^+)<1]$ or isovector $[B(2^+)>1]$ properties of the 2^+ state under consideration. The first $[2^+]_{RPA}$ state, which will be denoted by $[2^+_{is}]_{RPA}$, came out to have isoscalar nature and to be sensitive almost solely to the isoscalar quadrupole strength $\kappa_0^{(2)}$. The properties of the second $[2^+]_{RPA}$ state depend critically on the ratio $G^{(2)}/\kappa_0^{(2)}$ between the strengths of the quadrupole pairing and particle-hole interactions. The example of ^{136}Ba shown in Table II is illustrative of all nuclei. The ratio $B(2^+)$ increases dramati-

TABLE II. The sensitivity of the $M1$ and $E2$ transitions to the ratio $G^{(2)}/\kappa_0^{(2)}$ in ^{136}Ba.

$G^{(2)}/\kappa_0^{(2)}$	$B(E2;\text{g.s.}\rightarrow 2^+_{iv})_{RPA}$ $(e^2\,b^2)$	$B(M1;2^+_{iv}\rightarrow 2^+_{is})_{RPA}[\mu_N^2]$	$B(2^+_{iv})$
0	0.0032	0.042	0.58
0.85	0.011	0.24	22.6

cally with $G^{(2)}/\kappa_0^{(2)}$, more and more enforcing the isovector character of this $[2^+]_{RPA}$ state, which will be denoted by $[2^+_{iv}]_{RPA}$. The other properties of the state are also very sensitive to $G^{(2)}/\kappa_0^{(2)}$. Indeed, the strength $B(E2;\text{g.s.}\rightarrow[2^+_{iv}]_{RPA})$ increases with it thereby denoting an enhancement of the collectivity of the $[2^+_{iv}]_{RPA}$. A similar enhancement is obtained for the $[2^+_{iv}]_{RPA}\rightarrow[2^+_{is}]_{RPA}$ $M1$ transition.

Another quantitative test of the isospin nature of the lowest $[2^+]_{RPA}$ states is provided by the relative signs of the neutron and proton amplitudes ψ entering the RPA phonons (2.3). As shown in Table III, the proton-neutron amplitudes ψ of the main components of the $[2^+_{is}]_{RPA}$ phonon are in phase, while those of the $[2^+_{iv}]_{RPA}$ are out of phase. For an appropriate value of the ratio $G^{(2)}/\kappa_0^{(2)}$ $(=0.8\text{–}0.9)$, the RPA basis contains a collective isoscalar $[2^+_{is}]_{RPA}$ and a slightly collective isovector $[2^+_{iv}]_{RPA}$ state. The two states are mutually coupled via a relatively strong $M1$ transition. It is to be noticed that the ratio $G^{(2)}/\kappa_0^{(2)}$ used in the calculations is close to the self-consistent estimate made in Ref. [47]. The large $G^{(2)}$ has the effect of reducing the phonon backward amplitudes. This in turn implies a quenching of the ground state correlations and a reduction of the collectivity of $[2^+_{is}]_{RPA}$ state. We have computed the ratio $(\varphi^{i\lambda}_{jj'})^2/(\psi^{i\lambda}_{jj'})^2$ to estimate the ground state correlations. In the case of ^{136}Ba only few components contribute with appreciable backward amplitudes to the $[2^+_{is}]_{RPA}$ state. The largest value of such ratio is 0.06 for neutron and 0.03 for protons. The backward amplitudes contribute much less to the isovector $[2^+_{iv}]_{RPA}$ state. These estimates indicate that the contribution of the backward amplitudes $\varphi^{i\lambda}_{jj'}$ can be neglected unless they appear as leading terms. This is the case of the direct transitions from the ground to the two-phonon states [36–38]. Our result is consistent with the analysis carried out in Ref. [50], where it was shown that the effect of the ground state correlation in nuclei around closed shells is always small.

The choice of the phonon basis is dictated by the properties of the states to be determined. We included only phonons of positive parity, since negative parity phonons are not relevant to our low-lying positive parity QPM states. We considered phonons of multipolarity $\lambda=1\text{–}6$ and, for each λ, we included all phonons up to 5 MeV. Only for the 1^+ states the one-phonon space was enlarged up to an energy that includes the $M1$ resonance. Adding states above these energies does not affect the wave function (2.5). Since the QPM Hamiltonian mixes the multiphonon components differing by one phonon, the fragmentation of the two-phonon states is sensitive to the number of one- and three-phonon configurations. The most important three-phonon components are $[(2^+_{is}\otimes 2^+_{is})_I\otimes 2^+_{is}]_{JM}$ and $[(2^+_{is}\otimes 2^+_{is})_I\otimes 2^+_{iv}]_{JM}$.

IV. RESULTS

We adopted the outlined QPM formalism to generate the low-lying positive parity states and then compute the $E2$ and $M1$ mutual transition strengths in ^{136}Ba, ^{94}Mo, and ^{112}Cd. In all these nuclei one of the two open shells is occupied by two protons or two neutrons only. In our space, however, not only the valence but also the core particles are active. This allows one to account explicitly for the core polarizations that, otherwise, could have induced large correlations in the RPA ground state and, also, to minimize effects due to symmetry breakings, such as the violation of the particle number induced by the Bogoliubov transformation. In ^{136}Ba, for instance, the uncertainty on the neutron number is only 4.6%. Similar results are obtained for the other nuclei.

A. ^{136}Ba

Energy and structure of the low-lying states are shown in Table IV. Apart from few noncollective levels, such as the 2^+_{nc}, the states can be classified according to isospin and the RPA phonon content. They have in fact a dominant isoscalar

TABLE III. Structure of the first RPA phonons (only the largest components are given) and corresponding $B(2^+)$ ratios [see Eq. (3.1)] for ^{136}Ba.

λ^π_i	$\omega_{\lambda^\pi_i}$ (MeV)	Structure	$B(E2)\uparrow(e^2\,b^2)$	$B(2^+)$
2^+_{is}	0.95	$0.76(1h_{11/2})^2_n+0.72(2g_{7/2})^2_p$ $0.24(3s_{1/2}2d_{3/2})_n+0.43(2d_{5/2})^2_p$ $0.31(2d_{3/2})^2_n+0.23(1g_{7/2}2d_{3/2})_p$	0.51	0.0034
2^+_{iv}	2.009	$0.85(1h_{11/2})^2_n-0.98(1g_{7/2})^2_p$ $0.37(2d_{3/2})^2_n-0.17(2d_{5/2})^2_p$ $0.22(3s_{1/2}2d_{3/2})_n-0.1(1h_{11/2})^2_p$	0.011	22.6

TABLE IV. Energy and phonon structure of selected low-lying excited states in ^{136}Ba. Only the dominant components are presented.

State		E (keV)		Structure,%
T	J^π	Expt.	QPM	
IS	$2^+_{1,is}$	810	760	$77\%[2^+_{is}]_{RPA} + 19\%[2^+_{is}\otimes 2^+_{is}]_{RPA}$
	$2^+_{2,is}$	1551	1640	$48\%[2^+_{is}\otimes 2^+_{is}]_{RPA} + 17\%[2^+_{is}]_{RPA}$
	$4^+_{1,is}$	1866	1630	$60\%[2^+_1\otimes 2^+_1]_{RPA}$
IV	$2^+_{1,iv}$	2129	1850	$73\%[2^+_{iv}]_{RPA}$
	$1^+_{1,iv}$	2694	2800	$85\%[2^+_{is}\otimes 2^+_{iv}]_{RPA}$
	$2^+_{2,iv}$		3120	$51\%[2^+_{is}\otimes 2^+_{iv}]_{RPA}$
	$4^+_{1,iv}$		3230	$41\%[2^+_{is}\otimes 2^+_{iv}]_{RPA}$
	$3^+_{1,iv}$		3040	$90\%[2^+_{is}\otimes 2^+_{iv}]_{RPA}$
NC	$\mathbf{2}^+_{nc}$	2080	2370	Noncollective

or isovector multiphonon component exhausting at least 50% of the norm of the wave function. Nonetheless, the admixture with other components might be sizeable. In the second $2^+_{2,is}$, for instance, the dominant two-phonon piece $[2^+_{is}\otimes 2^+_{is}]_{RPA}$ gets admixed appreciably with the one-phonon $[2^+_{is}]_{RPA}$ (17%) and the three-phonon $[[2^+_{is}\otimes 2^+_{is}]_{IK}\otimes 2^+_{is}]_{JM}$ (10%).

The pronounced phonon structure, combined with isospin, leads to well defined $E2$ and $M1$ selection rules. As shown in Table V, the $E2$ strengths, computed with the effective charges $e^*_n = e^*_p = 0.1e$, are large for the one-phonon exchange transitions between the members of the isoscalar or the isovector group, and small for the boson forbidden transitions from isovector to isoscalar states. They are in very good agreement with the experimental data [28]. Only the strength of the $E2$ transition from the isoscalar $2^+_{2,is}$ to the ground state is four times larger than the experimental value, suggesting that the amplitude of the $[2^+_{is}]_{RPA}$ component (17%) is too large.

TABLE V. $E2$ transitions connecting some excited states in ^{136}Ba calculated in QPM. The experimental data are taken from Ref. [28].

	$B(E2;J_i\rightarrow J_f)$ $(e^2\,\mathrm{b}^2)$	Expt.	QPM
$\Delta T=0$	$B(E2;\mathrm{g.s.}\rightarrow 2^+_{1,is})$	0.400(5)	0.39
	$B(E2;\mathrm{g.s.}\rightarrow 2^+_{2,is})$	0.016(4)	0.08
	$B(E2;2^+_{2,is}\rightarrow 2^+_{1,is})$	0.09(4)	0.15
	$B(E2;4^+_{1,is}\rightarrow 2^+_{1,is})$		0.093
$\Delta T=0$	$B(E2;1^+_{1,iv}\rightarrow 2^+_{1,iv})$		0.066
	$B(E2;3^+_{1,iv}\rightarrow 2^+_{1,iv})$		0.066
	$B(E2;2^+_{2,iv}\rightarrow 2^+_{1,iv})$		0.04
	$B(E2;4^+_{1,iv}\rightarrow 2^+_{1,iv})$		0.036
$\Delta T=1$	$B(E2;\mathrm{g.s.}\rightarrow 2^+_{1,iv})$	0.045(5)	0.05
	$B(E2;2^+_{1,iv}\rightarrow 2^+_{1,is})$		0.003
	$B(E2;1^+_{1,iv}\rightarrow 2^+_{1,is})$		0.003
	$B(E2;1^+_{1,iv}\rightarrow 2^+_{2,is})$		0.0004

TABLE VI. QPM versus experimental $M1$ transitions between some excited states in ^{136}Ba. The experimental data are taken from Ref. [28].

	$B(M1;J_i\rightarrow J_f)(\mu^2_N)$	Expt.	QPM $g^s_{eff}=0.7$
$\Delta T=1$	$B(M1;2^+_{1,iv}\rightarrow 2^+_{1,is})$	0.26(3)	0.25
	$B(M1;g.s.\rightarrow 1^+_{1,iv})$	0.13(2)	0.17
	$B(M1;1^+_{1,iv}\rightarrow 2^+_{2,is})$	0.6(1)	0.18
	$B(M1;2^+_{2,iv}\rightarrow 2^+_{2,is})$		0.06
	$B(M1;3^+_{1,iv}\rightarrow 2^+_{2,is})$		0.07
	$B(M1;3^+_{1,iv}\rightarrow 4^+_{1,is})$		0.09
$\Delta T=0$	$B(M1;1^+_{1,iv}\rightarrow 2^+_{1,iv})$		8.10^{-4}

A reverse pattern holds for the $M1$ scheme (Table VI). The transitions between states of the same isospin are strongly suppressed, while the boson forbidden ones from isovector to isoscalar states are strongly favored. They are in good agreement with experiments with one puzzling exception. The computed $1^+_{1,iv}\rightarrow 2^+_{2,is}$ $M1$ transition strength is three times smaller than the measured one, suggesting that the amplitudes of the two-phonon components $[2^+_{is}\otimes 2^+_{is}]_{RPA}$ and $[2^+_{is}\otimes 2^+_{iv}]_{RPA}$ of the $2^+_{2,is}$ and $1^+_{1,iv}$ states, respectively, are not sufficiently large. It is not obvious, however, to find the way of enhancing these amplitudes without spoiling part of the $E2$ transition scheme.

The experiments have detected two direct $M1$ decays to the ground state. The first 1^+ level is described as a two-phonon state in agreement with the IBM picture. In fact, it is also strongly coupled to the two-phonon state $2^+_{2,is}$. The second 1^+_2, with energy of 3370 keV [28], is not coupled to $2^+_{2,is}$. It should have therefore a more composite structure not foreseen in the IBM. Our calculation yields a 1^+ state at 3.39 MeV followed by several others in the range 3.50–4.50 MeV, all very weakly coupled to the $2^+_{2,is}$ and decaying with non-negligible strengths to the ground state. All of them con-

TABLE VII. Energy and phonon structure of selected low-lying excited states in ^{94}Mo. Only the dominant components are presented.

State		E (keV)		Structure,%
T	J^π	Expt.	QPM	
IS	$2^+_{1,is}$	871	860	$93\%[2^+_{is}]_{RPA}$
	$2^+_{2,is}$	1864	1750	$82\%[2^+_{is}\otimes 2^+_{is}]_{RPA}$
	$4^+_{1,is}$	1573	1733	$82\%[2^+_{is}\otimes 2^+_{is}]_{RPA}$
IV	$1^+_{1,iv}$	3129	2880	$90\%[2^+_{is}\otimes 2^+_{iv}]_{RPA}$
	$2^+_{1,iv}$	2067	1940	$95\%[2^+_{iv}]_{RPA}$
	$2^+_{2,iv}$	2393	2730	$27\%[2^+_{is}\otimes 2^+_{iv}]_{RPA}$
	$2^+_{3,iv}$	2740	3014	$59\%[2^+_{is}\otimes 2^+_{iv}]_{RPA}$
	$4^+_{1,iv}$		3120	$64\%[2^+_{is}\otimes 2^+_{iv}]_{RPA}$
	$3^+_{1,iv}$	2965	2940	$87\%[2^+_{is}\otimes 2^+_{iv}]_{RPA}$
NC	$1^+_{2,iv}$		3550	$40\%[1^+_1]_{RPA}$

TABLE VIII. $E2$ transitions connecting some excited states in ^{94}Mo calculated in QPM. The experimental data are taken form Refs. [29,30].

	$B(E2;J_i\to J_f)$ $(e^2\,\mathrm{fm}^4)$	Expt.	QPM	IBM-2
$\Delta T=0$	$B(E2;\mathrm{g.s.}\to 2^+_{1,is})$	2030(40)	1978	2333
	$B(E2;\mathrm{g.s.}\to 2^+_{2,is})$	32(7)	35	0
	$B(E2;2^+_{2,is}\to 2^+_{1,is})$	720(260)	673	592
	$B(E2;4^+_{1,is}\to 2^+_{1,is})$	670(100)	661	592
$\Delta T=0$	$B(E2;2^+_{2,iv}\to 2^+_{1,iv})$		127	
	$B(E2;2^+_{3,iv}\to 2^+_{1,iv})$		266	
	$B(E2;1^+_{1,iv}\to 2^+_{1,iv})$	<690	374	556
	$B(E2;3^+_{1,iv}\to 2^+_{1,iv})$	$250\ ^{+310}_{-210}$ $(1.5\ ^{+1.2}_{-0.6})\times 10^3$	368	582
	$B(E2;4^+_{1,iv}\to 2^+_{1,iv})$		274	
$\Delta T=1$	$B(E2;\mathrm{g.s.}\to 2^+_{1,iv})$	230(30)	150	151
	$B(E2;\mathrm{g.s.}\to 2^+_{2,iv})$	27(8)	18	0
	$B(E2;\mathrm{g.s.}\to 2^+_{3,iv})$	83(10)	10	0
	$B(E2;1^+_{1,iv}\to 2^+_{1,is})$	30(10)	13	49
	$B(E2;3^+_{1,iv}\to 2^+_{1,is})$	9^{+25}_{-8}	12	

tain a small fraction (2%–3%) of the $J^\pi=1^+$ one phonon, which in turn contains a dominant spin-flip $(2d_{3/2}\otimes 2d_{5/2})$ two-quasiparticle configuration for protons and neutrons. The occurrence of these states in QPM supports the spin-flip nature of this second $M1$ transition. As we shall see, a quite analogous, more clear-cut, situation occurs in ^{94}Mo.

B. ^{94}Mo

For this nucleus the experimental information is quite rich [29–31] and theoretical microscopic studies are available. A calculation was performed in a truncated shell model space using a surface δ interaction [32], another was carried out by the present authors within the QPM [33]. In this latter paper we were forced to reduce strongly the spin-gyromagnetic ratio by using a quenching factor $g_s=0.3$ in order to get a satisfactory agreement with experiments. We have revisited the procedure in order to see if there are alternative, more consistent, ways of improving the agreement without artificially suppressing the spin contribution. To this purpose we changed slightly some Woods-Saxon parameters and reduced somewhat the $G^{(2)}/\kappa_0^{(2)}$ ratio to induce some quenching on the isovector transitions.

With respect to ^{136}Ba, the states have a more pronounced phonon structure (Table VII) that leads to even sharper selection rules. Once again, we notice (Table VIII) strong one-phonon exchange transitions between isoscalar or isovector states and very weak boson forbidden transitions from isovector to isoscalar states. The $E2$ reduced transition probabilities, computed with effective charges $e_n^*=e_p^*=0.2e$, are in excellent agreement with experiments.

Equally satisfactory is the scheme of the $M1$ transitions (Table IX). The only noticeable discrepancy concerns the two $2^+_{1,iv}\to 2^+_{1,is}$ and $1^+_{1,iv}\to 2^+_{2,is}$ transitions, which are somewhat overestimated. The same transition strengths are underestimated by the IBM-2 [29], where spin is ignored, and are well reproduced by a shell model calculation [32]. This, however, used the smaller gyromagnetic factor $g^{(s)}_{eff}=0.57g^{(s)}_{free}$ and was carried out in a severely truncated

TABLE IX. $M1$ transitions connecting some excited states in ^{94}Mo calculated in QPM. The experimental data are taken from Refs. [29,30].

	$B(M1;J_i\to J_f)(\mu_N^2)$	Expt.	QPM		IBM-2
			$g^s_{eff}=0.7g^s_{free}$	$g^s_{eff}=0.0g^s_{free}$	
$\Delta T=1$	$B(M1;1^+_{1,iv}\to 2^+_{2,is})$	0.43(5)	0.75	0.22	0.36
	$B(M1;2^+_{1,iv}\to 2^+_{1,is})$	0.48(6)	0.72	0.23	0.30
	$B(M1;2^+_{2,iv}\to 2^+_{2,is})$		0.10	0.034	
	$B(M1;2^+_{3,iv}\to 2^+_{2,is})$	0.35(11)	0.24	0.072	0.1
	$B(M1;3^+_{1,iv}\to 2^+_{2,is})$	$0.24^{+0.14}_{-0.07}$	0.34	0.10	0.18
	$B(M1;3^+_{1,iv}\to 4^+_{1,is})$	$0.074^{+0.044}_{-0.019}$	0.26	0.08	0.13
	$B(M1;4^+_{1,iv}\to 4^+_{1,is})$	0.8(2)	0.75	0.23	
$\Delta T=1$	$B(M1;1^+_{1,iv}\to \mathrm{g.s.})$	0.16(1)	0.14	0.09	0.16
	$B(M1;1^+_{1,iv}\to 2^+_{1,is})$	0.007^{+6}_{-2}	6.10^{-4}	5.10^{-3}	0
	$B(M1;2^+_{2,iv}\to 2^+_{1,is})$	0.07	0.001	0.002	0
	$B(M1;2^+_{3,iv}\to 2^+_{1,is})$	0.03	0.013	0.005	0
	$B(M1;3^+_{1,iv}\to 2^+_{1,is})$	$0.01^{+0.012}_{-0.006}$	0.006	0.0025	0
$\Delta T=0$	$B(M1;1^+_{1,iv}\to 2^+_{1,iv})$	<0.05	3.10^{-6}	2.10^{-5}	0
	$B(M1;3^+_{1,iv}\to 2^+_{1,iv})$	$0.021^{+0.035}_{-0.014}$ $0.09^{+0.07}_{-0.03}$	2.10^{-5}	9.10^{-6}	0
	$B(M1;2^+_{2,is}\to 2^+_{1,is})$	0.06	0.006	0.004	0
	$B(M1;1^+_{nc}\to \mathrm{g.s.})$	0.046(18)	0.04	0.009	

space, which excludes part of the spin configurations.

This brief comparative analysis has implicitly emphasized the role of spin. This is specially noticeable in the $4^+_{1,iv} \rightarrow 4^+_{1,is}$ $M1$ transition, whose experimental strength, largely overestimated in shell model [32], is well reproduced in QPM due to the appreciable spin contribution. Such a role emerges also from the analysis of the two direct $M1$ decays to the ground state observed also in ^{94}Mo. The calculation reproduces satisfactorily the strengths of both $M1$ transitions. At the same time, it shows that the difference between the two 1^+ initial states is more marked than in ^{136}Ba. In fact, the lowest $1^+_{1,iv}$ has a dominant two-phonon isovector component responsible for the (boson forbidden) decay. It is the counterpart of the IBM mixed-symmetry 1^+ state, decaying to the ground state in the $O(6)$ limit [29]. The second 1^+_2 instead has a composite structure and contains a sizeable $[1^+]_{RPA}$ with the dominant spin-flip quasiparticle configuration $(2p_{3/2} \otimes 2p_{1/2})$ responsible for the decay to the ground state. This transition is out of the domain of the IBM.

C. ^{112}Cd

^{112}Cd was one of the first nuclei explored experimentally for the search of mixed-symmetry states in nearly spherical nuclei [26,27]. Its low-lying spectrum is more complex than in ^{94}Mo and ^{136}Ba. The vibrational band includes up to three-phonon levels [27], but also two intruders of spin 0^+ and 2^+ within the two-phonon multiplet. Due to its large number of valence neutrons, this nucleus is at the border of the range of validity of the QPM. Indeed, the large effective charges $e^*_n = e^*_p = 0.5e$ produced by the fit imply strong renormalization effects not accounted for completely by our QPM space. Our predictions have therefore only a semiquantitative validity.

The overall picture is the same as in the other nuclei under exam. We get a low-lying 2^+ state with a dominant one-phonon component (81%) promoting its strong $E2$ decay, and a second 2^+ of energy 1.66 MeV with a large two-phonon component $[2^+_{is} \otimes 2^+_{is}]_{RPA}$ (53%), responsible for its strong $E2$ transition to the lowest $2^+_{1,is}$. We obtain also a third (isovector one-phonon) $2^+_{1,iv}$, of energy 1.931 MeV, $M1$ coupled to the isoscalar $2^+_{1,is}$ with a strength $B(M1; 2^+_{1,iv} \rightarrow 2^+_{1,is}) = 0.25\ \mu_N^2$. A level of the same energy was observed [26], although with a strength five times smaller than the QPM (and IBM) value. We mention, finally, the prediction at 2.97 MeV of a 1^+ state with 95% of the two-phonon $[2^+_1 \otimes 2^+_2]_{RPA}$, carrying the strength $B(M1; 1^+_{1,iv} \rightarrow \text{g.s.}) = 0.17\ \mu_N^2$.

Similar $M1$ and $E2$ transition schemes were predicted for ^{144}Nd [51] and $^{122-130}$Te [52]. They are not yet supported by sufficient experimental data.

V. CONCLUSIONS

According to our findings, the building blocks of our QPM multiphonon low-lying states in nuclei near shell closure are the first and second $[2^+]_{RPA}$ states. The first couples strongly to the ground state through the isoscalar $E2$ operator, the second through the isovector one. This occurs at low energy only for a sufficiently strong proton-proton and neutron-neutron quadrupole pairing interaction.

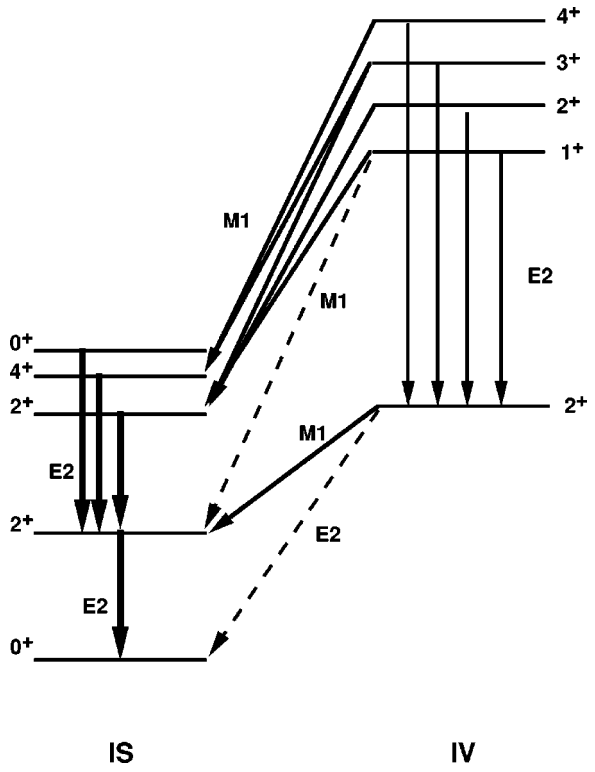

FIG. 1. Schematic picture of the level and transition scheme. The dashed arrows indicate the weak transitions.

The resulting low-lying QPM states can be classified into two groups, composed, respectively, of isoscalar and isovector states. All these states have a single dominant component with a given number of phonons. This feature makes possible a further classification of the states of each group according to the number of phonons and leads to well defined selection rules. A schematic picture of the level and transition scheme is given in Fig. 1. We obtain appreciable $E2$ strengths only for transitions connecting states differing by one phonon. They are very large when the states involved in the $E2$ transition are isoscalar, large for transitions between isovector states, small for transitions between states of different isospin. On the contrary, the $M1$ operator couples strongly only states of different isospin with an equal number of phonons. We should point out that these transitions are promoted by the scattering piece of the $M1$ operator ignored in most multiphonon calculations.

The picture emerging from the present calculation and outlined in Fig. 1 seems to be a general feature of nuclei near shell closure and is consistent with the IBM scheme. Our isoscalar and isovector states correspond to fully symmetric and mixed-symmetry IBM states.

These mixed-symmetry states can be put in close connection with the scissors mode. There is, in fact, no clear cut distinction between mixed-symmetry and scissorslike states. Both kinds of states have the same signature, a strong $M1$ coupling with the symmetric states. Such a close correspondence can be extended further through the following heuris-

tic argument. We can obtain a mixed-symmetry state from a symmetric one by replacing one symmetric quadrupole operator $Q_s = Q_p + Q_n$ with the antisymmetric one $Q_m = Q_p - Q_n$. Such a transformation is induced by the action of the scissors operator $S_\mu = J^p_\mu - J^n_\mu$ on symmetric states in spherical or nearly spherical nuclei giving rise to a multiplet of state of the same structure. When acting, for instance, on the symmetric two-phonon states, the scissors operator generates a multiplet of mixed-symmetry states. In ^{94}Mo, for instance, the computed summed strength of the multiplet $\{1^+_{1,iv}, 2^+_{2,iv}, 3^+_{1,iv}, 4^+_{1,iv}\}$ is $\Sigma_n B_n(M1) = 2.18\mu_N^2$, rather close to the experimental sum $\Sigma_n B_n(M1) \simeq 1.82\mu_N^2$.

With respect to the algebraic approach, the QPM provides information on the spin correlations present in these states. We have found, specially in ^{94}Mo, that the spin contribution is comparable to the orbital one in the strongest $M1$ transitions. The overestimation of the strengths of two $M1$ transitions with respect to the experiments suggests that one should change slightly and selectively the parameters entering into the one-body potential in order to reduce slightly the amplitudes of the spin-flip components of some selected QPM wave functions. Doing now such a fine tuning adjustment would be premature. We need first experimental information on the detailed structure of the $M1$ resonance.

The spin degree of freedom plays a dominant role in some states, such as the second 1^+, which has a composite structure and includes spin-flip configurations with appreciable amplitudes through which it can be coupled to the ground state. Such a state falls outside the multiphonon picture drawn above.

In summary, the generally good agreement with experiments indicates that the QPM calculation provides a realistic description of the low-lying states in nuclei near the shell closure. The level and transition scheme obtained is consistent with the picture provided by the algebraic IBM and appears to be a general feature of nuclei near shell closure. The calculation, however, points out the significant role played by the spin in determining the pattern of the $M1$ transitions.

ACKNOWLEDGMENTS

This work was partly supported by the Italian Ministry of Research and Technology (MURST) through the PRIN99 funds and by the Bulgarian Science Foundation (Contract No. Ph. 801). The authors thank N. Tsoneva for assistance in the calculation and U. Kneissl for useful information and discussions.

[1] D. Bohle, A. Richter, W. Steffen, A.E.L. Dieperink, N. Lo Iudice, F. Palumbo, and O. Scholten, Phys. Lett. **137B**, 27 (1984).
[2] N. Lo Iudice and F. Palumbo, Phys. Rev. Lett. **41**, 1532 (1978).
[3] E. Lipparini and S. Stringari, Phys. Lett. **130B**, 139 (1983).
[4] R.R. Hilton, Z. Phys. A **316**, 121 (1984).
[5] F. Iachello, Nucl. Phys. **A358**, 89c (1981).
[6] A.E.L. Dieperink, Prog. Part. Nucl. Phys. **9**, 121 (1983).
[7] A. Richter, Prog. Part. Nucl. Phys. **34**, 261 (1995), and references therein.
[8] U. Kneissl, H.H. Pitz, and A. Zilges, Prog. Part. Nucl. Phys. **37**, 349 (1996), and references therein.
[9] N. Lo Iudice, Phys. Part. Nucl. **28**, 556 (1997), for a review and references.
[10] W. Ziegler, C. Rangacharyulu, A. Richter, and C. Spieler, Phys. Rev. Lett. **65**, 2515 (1990).
[11] C. Rangacharyulu, A. Richter, H.J. Wörtche, W. Ziegler, and R.F. Casten, Phys. Rev. C **43**, R949 (1991).
[12] N. Pietralla, P. von Brentano, R.-D. Herzberg, U. Kneissl, J. Margraf, H. Maser, H.H. Pitz, and A. Zilges, Phys. Rev. C **52**, R2317 (1995).
[13] P. von Neumann-Cosel, J.N. Ginocchio, H. Bauer, and A. Richter, Phys. Rev. Lett. **75**, 4178 (1995).
[14] N. Pietralla, P. von Brentano, R.-D. Herzberg, U. Kneissl, N. Lo Iudice, H. Maser, H.H. Pitz, and A. Zilges, Phys. Rev. C **58**, 184 (1998).
[15] J. Enders, H. Kaiser, P. von Neumann-Cosel, C. Rangacharyulu, and A. Richter, Phys. Rev. C **59**, R1851 (1999).
[16] A. Faessler, Nucl. Phys. **85**, 653 (1966).
[17] A. Faessler and R. Nojarov, Phys. Lett. **166B**, 367 (1986).
[18] R. Nojarov and A. Faessler, J. Phys. G **13**, 337 (1987).
[19] T. Otsuka, A. Arima, and Iachello, Nucl. Phys. **A309**, 1 (1978).
[20] W.D. Hamilton, A. Irbïack, and J.P. Elliott, Phys. Rev. Lett. **53**, 2469 (1984).
[21] G. Molnár, R.A. Gatenby, and S.W. Yates, Phys. Rev. C **37**, 898 (1988).
[22] R. De Leo *et al.*, Phys. Rev. C **53**, 2718 (1996).
[23] A. Giannatiempo, A. Nannini, A. Perego, P. Sona, and D. Cutoui, Phys. Rev. C **53**, 2718 (1996).
[24] W.J. Vermeer, C.S. Lim, and R.H. Spear, Phys. Rev. C **38**, 2982 (1988).
[25] B. Fazekas, T. Belgya, G. Molnár, A. Veres, R.A. Gatenby, Y.W. Yates, and T. Otsuka, Nucl. Phys. **A548**, 249 (1992).
[26] P.E. Garrett, H. Lehmann, C.A. McGrath, Minfang Yeh, and S.W. Yates, Phys. Rev. C **54**, 2259 (1996).
[27] H. Lehmann, P.E. Garrett, J. Jolie, C. A. McGrath, Minfang Yeh, and S. W. Yates, Phys. Lett. B **387**, 259 (1996).
[28] N. Pietralla, D. Belic, P. von Brentano, C. Fransen, R.-D. Herzberg, U. Kneissl, H. Maser, P. Matschinsky, A. Nord, T. Otsuka, H.H. Pitz, V. Werner, and I. Wiendenöver, Phys. Rev. C **58**, 796 (1998).
[29] N. Pietralla, C. Fransen, D. Belic, P. von Brentano, C. Friessner, U. Kneissl, A. Linnemann, A. Nord, H.H. Pitz, T. Otsuka, I. Schneider, V. Werner, and I. Wiedenlòver, Phys. Rev. Lett. **83**, 1303 (1999).
[30] N. Pietralla, C. Fransen, P. von Brentano, A. Dewald, A. Filzler, C. Friesner, and J. Gableske, Phys. Rev. Lett. **84**, 3775 (2000).
[31] C. Fransen, N. Pietralla, P. von Brentano, A. Dewald, J. Gableske, A. Gade, A. Lisetskiy, and V. Werner, Phys. Lett. B **508**, 219 (2001).
[32] A.F. Lisetskiy, N. Pietralla, C. Fransen, R.V. Jolos, and P. von

Brentano, Nucl. Phys. **A677**, 1000 (2000).
[33] N. Lo Iudice and Ch. Stoyanov, Phys. Rev. C **62**, 047302 (2000).
[34] V.G. Soloviev, *Theory of Atomic Nuclei: Quasiparticles and Phonons* (Institute of Physics, Bristol, 1992).
[35] S.T. Beliaev and V.G. Zelevinsky, Nucl. Phys. **39**, 582 (1962).
[36] M. Grinberg and Ch. Stoyanov, Nucl. Phys. **A535**, 231 (1994).
[37] V. Yu. Ponomarev, Ch. Stoyanov, N. Tsoneva, and M. Grinberg, Nucl. Phys. **A635**, 470 (1998).
[38] T.K. Dinh, M. Grinberg, and Ch. Stoyanov, J. Phys. G **18**, 329 (1992); M. Grinberg, Ch. Stoyanov, and N. Tsoneva, Phys. Part. Nucl. **29**, 606 (1998).
[39] S. Gales, Ch. Stoyanov, and A. I. Vdovin, Phys. Rep. **166**, 125 (1988).
[40] V. A. Chepurnov, Yad. Fiz. **5**, 955 (1967) [Sov. J. Nucl. Phys. **6**, 696 (1968)].
[41] K. Takeuchi and P. A. Moldauer, Phys. Lett. **28B**, 384 (1969).
[42] A. Bohr and B.R. Mottelson, *Nuclear Structure* (Benjamin, New York, 1975), Vol. 2, Chap. 6.
[43] M.S. Fayache, S. Shelly Sharma, and L. Zamick, Phys. Lett. B **357**, 1 (1995).
[44] R. Nojarov, A. Faessler, and M. Dingfelder, Phys. Rev. C **51**, 2449 (1995).
[45] E. Lipparini and A. Richter, Phys. Lett. **144B**, 13 (1984).
[46] S.T. Belyaev, J. Nucl. Phys. (U.S.S.R.) **4**, 936 (1966) [Sov. J. Nucl. Phys. **4**, 671 (1967)].
[47] H. Sakamoto and T. Kishimoto, Phys. Lett. B **245**, 321 (1990).
[48] T. Kubo, H. Sakamoto, K. Kammuri, and T. Kishimoto, Phys. Rev. C **54**, 2331 (1996).
[49] R. Nikolaeva, Ch. Stoyanov, and A.I. Vdovin, Europhys. Lett. **8**, 117 (1989).
[50] W. Nawrocka-Rybarska, O. Stoyanova, and Ch. Stoyanov, Yad. Fiz. **33**, 1494 (1980) [Sov. J. Nucl. Phys. **33**, 802 (1981)].
[51] Ch. Stoyanov, N. Lo Iudice, N. Tsoneva, and M. Grinberg, Atom. Nucl. **64**, 1223 (2001).
[52] R. Schwengner *et al.*, Nucl. Phys. **A620**, 277 (1996).